

# Analysis of Chiral and Achiral Medium Based Coplanar Waveguide Using Improved Full Generalized Exponential Matrix Technique

Djamel SAYAD<sup>1</sup>, Chemseddine ZEBIRI<sup>2</sup>, Issa ELFERGANI<sup>3</sup>, Jonathan RODRIGUEZ<sup>4</sup>,  
Raed ABD-ALHAMEED<sup>5</sup>, Fatiha BENABDELAZIZ<sup>6</sup>

<sup>1</sup> Dept. of Electrical Engineering, University 20 Aout 1955-Skikda, Skikda, Algeria

<sup>2</sup> Dept. of Electronics, University of Ferhat Abbas, Sétif -1-, 19000 Sétif, Algeria

<sup>3</sup> Instituto de Telecomunicações, Campus Universitário de Santiago, Aveiro, 3810-193, Portugal

<sup>4</sup> Faculty of Computing, Engineering and Science, University of South Wales, Pontypridd, CF37 1DL, UK

<sup>5</sup> School of Electrical Engineering and Computer Science, University of Bradford, BD71DP, UK

<sup>6</sup> Dept. of Electronics, University Mentouri, Constantine 1, Algeria

d.sayad@univ-skikda.dz, czebiri@univ-setif.dz, i.t.e.elfergani@av.it.pt, jonathan.rodriguez@southwales.ac.uk,  
R.A.A.Abd@bradford.ac.uk, benabdelaziz2003@yahoo.fr

Submitted May 20, 2020 / Accepted August 6, 2020

**Abstract.** *In this work, an analytical study of the electromagnetic propagation in a complex medium-based suspended three-layer coplanar waveguide (CPW) is carried out. The study aims at a numerical calculation of the dominant hybrid mode complex propagation constant in the CPW printed on a bianisotropic substrate. The herein considered bianisotropy is characterized by full  $3 \times 3$  tensors of permittivity, permeability and magnetoelectric parameters. The study is based on the numerical derivation of the Green's functions of such a complex medium in the spectral domain. The study is carried out using the Full Generalized Exponential Matrix Technique based on matrix-shaped compact mathematical formulations. The Spectral Method of Moments (SMoM) and the Galerkin's procedure are used to solve the resulting homogeneous system of equations. The effect of the chiral and achiral bianisotropy on the complex propagation constant is particularly investigated. Good agreements with available data for an anisotropic-medium-based suspended CPW structure are achieved. Various cases of chiral and achiral bianisotropy have been investigated, and particularly, the effect on the dispersion characteristics is presented and compared with cases of isotropic and bianisotropic Tellegen media.*

## Keywords

CPW, chiral and achiral, Tellegen, full-GEMT, complex propagation constant

## 1. Introduction

As technology advances and due to the introduction of new synthetic electronic materials, microwave devices are getting smarter and smarter [1]. Hence, adding a degree of freedom in the design of these devices would be very beneficial in terms of miniaturization, flexibility, losslessness and ultra-wideband characteristics. These new contributions make it possible, nowadays, to face and solve several problems such as those related to high performance devices that may respond to the needs of modern technologies. Electromagnetic theories have brought upon considerable achievements in the field of this class of complex synthetic materials. Bianisotropic media have offered a promising alternative to conventional microwave and optical components due to their ability to provide new intrinsic electromagnetic properties not actually known in natural materials. These particular properties are due to the additional degree of freedom, they offer, manifested by the magnetoelectric coupling explicitly described by the general constitutive relations. The degrees of freedom available in the frame of complex synthetic materials allowed obtaining some combinations of inclusions and host dielectrics, giving rise to new unusual materials. In 2000, San Diego group managed to fabricate for the first time what is now referred to as “*metamaterial*”; a material with a negative refractive index [2], [3]. Chiral materials also have constantly received considerable attention over the last four decades [4]. They are realized using many fabrication techniques where the most common ones consist in

dispersing random helices or cranks in a dielectric host medium [5–7].

Over the last three decades, the electromagnetism of bianisotropic media has gained a great deal of interest from scientists and researchers [8]. Recently, as the science of materials has tremendously advanced, the concept of bianisotropic media has reemerged as a major development player in the field of microwave and optic technologies [9–11]. The electromagnetic properties of bianisotropic media have to be analyzed to perceive their exotic characteristics. By knowing the intrinsic physical properties of complex media, designers can predict their electromagnetic response, which may help in developing inventive microwave devices. Several studies have been carried out for the characterization of the electromagnetic behavior of these materials [12–16]. However, the complex mathematical modeling of these media constitutes a real challenge in the characterization of microwave components. Various techniques have been used to extract the effective constitutive parameters of bianisotropic materials, such as stepwise method, S-parameters method, resonator method, coaxial probe method, free-space characterization method, rectangular waveguide measurements and recursive algorithms [17], [18]. On the other hand, several studies have been carried out for the analysis of planar structures, their dispersion and radiation characteristics in the case of simple or complex substrate media, using numerical and analytical methods [1], [12–15], [19–24]. In [19], a uniaxial bianisotropic based antenna structure is studied, the effect of the chirality on the resonant frequency and bandwidth are investigated.

In [25], both gyrotropic anisotropy and chirality are introduced in some composite fin-line structures. The propagation characteristics are investigated using the generalized exponential technique in the spectral domain combined with Galerkin's method. Numerical calculations are performed so as to examine the combined effects of changing different variables associated with the gyrotropy and chirality parameters on the dominant mode propagation constant.

In [1] and [26], the case of a complex gyrotropic anisotropy and a complex bianisotropic medium were considered, respectively. Some necessary conditions were taken into account, in both studies, to ensure the TE-TM decoupling for the characterization of a transmission line structure. Heavy calculations had been dealt with, using the spectral moment method. In [27], the cases of complex bianisotropic media are treated. The calculations were developed using the GEM technique in the Fourier domain. The mathematical formulations were less complex compared to the previous studies, however, the problem was the failure in the solution method where it did not give solutions for full matrices of the magnetoelectric parameters  $\xi$  and  $\eta$ ; only special cases were investigated for a transmission line structure. In [23], the case of general complex bianisotropic media for a CPW structure was considered. The introduction of a new accelerating proce-

dure, in the solution technique based on the GEM technique, helped to overcome the drawbacks of the solution method used in [27]. New results were obtained for various cases of Tellegen media. This has incited us to further exploit the GEM technique and to analyze more complex multilayer structures implanted on more complex media such as chiral and achiral materials.

In the present work, a modelling of the wave propagation in a general bianisotropic medium with full tensors of permittivity, permeability and magnetoelectric parameters is carried out, no conditions are imposed on the constitutive parameters. This case of medium is considered, herein, for implementing a three-layer coplanar waveguide (CPW) structure. The effect of the chiral and achiral bianisotropy on the complex propagation constant is particularly investigated including the loss factor. In [25], the study did not consider the losses, only the influences of chirality on the phase constant are investigated, where it is shown that they are just diverse.

This study is conducted through the numerical derivation of the dyadic Green's functions for such a guiding structure developed in the Full-GEM method. This method is opted for in order to avoid developing complex mathematical expressions of the Green's functions and dealing with highly complex theoretical equations [23], [27], [28]. Solutions are tailored to the studied structure considering appropriate boundary conditions using the Spectral Galerkin's Method of Moments (SGMoM); a method that is extensively used in analyzing microwave planar structures [16], [21], [22], [29–33]. The SGMoM is supplemented with an accelerating procedure developed in the GEMT [23] to speed up searching for the exact solution. This has helped us to obtain accurate solutions for the relative effective permittivity  $(\beta/\kappa_0)^2$  and losses  $(\alpha/\kappa_0)^2$  with tolerable computing time.

## 2. Mathematical Formulation

The geometry and parameters of the considered shielded CPW are shown in Fig. 1. The coplanar structure is supported by a bianisotropic medium of width  $d_2$  sandwiched between two isotropic dielectric layers. The bianisotropic layer is characterized by full 3×3-magnetoelectric tensors expressing the cross coupling between the electric

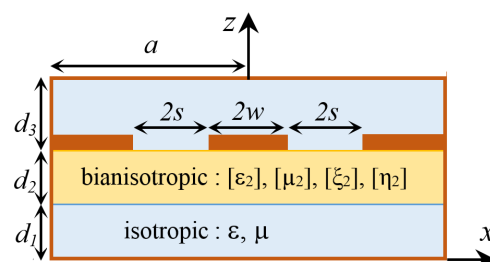


Fig. 1. Configuration of the shielded multilayer CPW structure, ( $a = 10$  mm,  $d_1 = 4.5$  mm,  $d_2 = 1$  mm,  $d_3 = 4.5$  mm,  $w = 1$  mm,  $s = 1$  mm,  $\epsilon_r = 2.53$ ,  $\mu_r = 1$ ).

and magnetic fields. Assuming the time-harmonic dependence  $\exp(j\omega t)$  of the electromagnetic fields propagating in the  $y$ -direction. Thin metal strips are assumed to be perfect electric conductors.

In complex media, the constitutive equations establish relations between field vectors completing Maxwell's equations, which can describe electromagnetic properties of media in a wide frequency range up to optical region and realize self consistent systems [34]. A bianisotropic material, in its general form, exhibits a cross coupling between the electric and magnetic fields. The appropriate constitutive relations are stated as follows [22], [27], [31].

$$\begin{aligned} \mathbf{D} &= \varepsilon_0 [\boldsymbol{\varepsilon}] \mathbf{E} + \sqrt{\varepsilon_0 \mu_0} [\boldsymbol{\xi}] \mathbf{H}, \\ \mathbf{B} &= \mu_0 [\boldsymbol{\mu}] \mathbf{H} + \sqrt{\varepsilon_0 \mu_0} [\boldsymbol{\eta}] \mathbf{E} \end{aligned} \quad (1)$$

where  $[\boldsymbol{\varepsilon}]$ : the relative permittivity,  $[\boldsymbol{\mu}]$ : the relative permeability and  $[\boldsymbol{\xi}]$  and  $[\boldsymbol{\eta}]$ : the cross coupling or magnetoelectric parameters given in a tensor form by

$$\boldsymbol{\psi} = \begin{bmatrix} \psi_{xx} & \psi_{xy} & \psi_{xz} \\ \psi_{yx} & \psi_{yy} & \psi_{yz} \\ \psi_{zx} & \psi_{zy} & \psi_{zz} \end{bmatrix} \quad (2)$$

where  $\psi$  stands for  $[\boldsymbol{\varepsilon}]$ ,  $[\boldsymbol{\mu}]$ ,  $[\boldsymbol{\xi}]$  or  $[\boldsymbol{\eta}]$ .

The magnetoelectric parameters are complex quantities, they are generally given by [34], [35].

$$\boldsymbol{\xi} = \boldsymbol{\chi} - j\boldsymbol{\kappa}, \quad \boldsymbol{\eta} = \boldsymbol{\chi} + j\boldsymbol{\kappa} \quad (3)$$

where  $\boldsymbol{\kappa}$  is the chirality parameter and  $\boldsymbol{\chi}$  the Tellegen parameter.

In [34], the symmetry of the constitutive tensors were mathematically investigated. Tables of possible combinations of constitutive tensors elements describing groups of symmetry are presented. These groups of symmetry may serve as a basis for synthesis of new artificial materials for advanced electromagnetic applications. Some restrictions may be imposed on the constitutive tensors for case simplification. For example, for lossless media, the following conditions are necessary  $[\boldsymbol{\mu}] = [\boldsymbol{\mu}^*]^t$ ,  $[\boldsymbol{\varepsilon}] = [\boldsymbol{\varepsilon}^*]^t$ ,  $[\boldsymbol{\xi}] = [\boldsymbol{\xi}^*]^t$  and for nonmagnetic media, the tensors  $[\boldsymbol{\xi}]$  and  $[\boldsymbol{\eta}]$  are always coupled [34].

The generalized exponential matrix technique adopts a mathematical formulation of the electromagnetic field expressions based on a matrix form. This formulation has the advantage of avoiding excessive mathematical equation development and skipping unnecessary explicit calculation steps. This can reduce the processed data redundancy in the solution method and helps in reducing the real computational time. The reduced mathematical equation manipulation is a highly desirable feature in mathematical modelling of complex structures implanted on complex substrates. Consequently, the generalized exponential matrix technique is optimal for solving the basic equations modelling problems related to propagation and radiation in the presence of multilayer bianisotropic media that require heavy

mathematical calculations in microwave and optical domains. The use of the GEMT is especially important in avoiding any *a priori* specific assumptions on the constitutive parameters to lighten calculations. Hence, general full  $3 \times 3$  constitutive parameter tensors are considered and complex propagation constant, considering losses, is solved for.

The basic principle of the GEMT is to express the transverse electromagnetic field components as functions of their derivatives coupled in four first-order differential equations given in the Fourier domain as follows [27], [28]:

$$\frac{\partial [\tilde{\mathbf{F}}^{(i)}(\alpha, \beta, z)]}{\partial z} = [\mathbf{P}^{(i)}]_{4 \times 4} [\tilde{\mathbf{F}}^{(i)}(\alpha, \beta, z)] \quad (4)$$

where  $z$  is the stratification axis,  $\alpha$  and  $\beta$  are the Fourier variables corresponding to the space domain wavenumbers  $\kappa_x$  and  $\kappa_y$ . The matrix  $[\mathbf{P}^{(i)}]$  denotes a  $z$ -independent  $4 \times 4$ -matrix, expressed in terms of the constitutive parameters elements given in [23].

The function  $\tilde{\mathbf{F}}^{(i)}$  stands for the  $x$ - and  $y$ -electromagnetic field components in the  $i^{\text{th}}$  layer of the stratified CPW structure given by a  $4 \times 1$ -matrix:

$$[\tilde{\mathbf{F}}^{(i)}(\alpha, \beta, z)] = \begin{bmatrix} \tilde{E}_x^{(i)}(\alpha, \beta, z) \\ \tilde{E}_y^{(i)}(\alpha, \beta, z) \\ \tilde{H}_x^{(i)}(\alpha, \beta, z) \\ \tilde{H}_y^{(i)}(\alpha, \beta, z) \end{bmatrix}. \quad (5)$$

Equation (4) admits a general solution in terms of the transition  $4 \times 4$ -matrix  $\mathbf{T}(\kappa_x, \kappa_y, z)$  of the form

$$[\tilde{\mathbf{F}}^{(i)}(\alpha, \beta, z_i)] = [\mathbf{T}(\kappa_x, \kappa_y, z)]_{4 \times 4} [\tilde{\mathbf{F}}^{(i)}(\alpha, \beta, z_{i-1})]. \quad (6)$$

The most important step in solving these reduced matrix-based equations using the GEMT is the generation of the transition matrix  $\mathbf{T}$  of the stratified system given by

$$[\mathbf{T}(\kappa_x, \kappa_y, z)] = \exp([\mathbf{P}] \cdot z). \quad (7)$$

The transition matrix  $\mathbf{T}(\kappa_x, \kappa_y, z)$  is calculated in the formulation of the GEMT by means of the Cayley Hamilton theorem. For more details one can refer to [28]. The total transition matrix is then obtained as the product of the different transition matrices of the different layers of the structure. This technique exhibits a compact matrix form with the advantage of being easily inserted in the calculation code.

In [23], the study focused mainly on the improvement of the GEMT technique where an acceleration procedure was implemented to improve the technique in terms of convergence and accuracy. Important and original results were found for the complex bianisotropic with real valued magnetoelectric parameters (Tellegen media). This has incited us to consider, in the present work, the case of imaginary valued magnetoelectric parameters cases (chiral and achiral media).

### 3. Method of Solution

By applying the boundary conditions, the expressions of the electric and magnetic tangential components are evaluated at the interface air-dielectric in terms of the tangential current densities on the strips  $\tilde{j}_x$  and  $\tilde{j}_y$ . The Green's tensor elements  $G_{ij}(\alpha_n, \beta)$  for the studied structure are calculated and arranged in a matrix form according to the following system of equations:

$$\begin{bmatrix} \tilde{j}_x \\ \tilde{j}_y \end{bmatrix} = \frac{1}{\Delta_G} \begin{bmatrix} G_{22}(\alpha_n, \beta) & -G_{12}(\alpha_n, \beta) \\ -G_{21}(\alpha_n, \beta) & G_{11}(\alpha_n, \beta) \end{bmatrix} \begin{bmatrix} \tilde{E}_x \\ \tilde{E}_y \end{bmatrix} \quad (8)$$

with  $\Delta_G = G_{11}G_{22} - G_{12}G_{21}$  and  $\alpha_n$  is the discrete Fourier transform variable with  $n$  the Fourier number of terms  $n = 1, 2, 3, \dots, N$ .

For resolving the problem, the SGMoM is applied [25], [27], [31], [36]. The method consists in expanding the field components in terms of sets of basis functions  $\tilde{E}_x$  and  $\tilde{E}_y$  with unknown coefficients  $a_p$  and  $b_q$ :

$$\tilde{E}_x(x) = \sum_{p=1}^{\infty} a_p \tilde{E}_{x,p}, \quad (9.a)$$

$$\tilde{E}_y(x) = \sum_{q=1}^{\infty} b_q \tilde{E}_{y,q}. \quad (9.b)$$

By substituting in (8) and taking the inner product with  $\tilde{E}_x$  and  $\tilde{E}_y$ , and using the Galerkin procedure, taking into account the condition that the tangential electric fields vanish over the conducting strips and the current densities are non-zero over the strips only, hence, the resulting inner product is zero everywhere.

$$\left\langle \tilde{j}_y, \tilde{E}_{y,q} \right\rangle = \frac{1}{2a\Delta_G} \left[ \int_{-a}^{+a} G_{11}(\alpha_n, \beta) \sum_{q=1}^{\infty} b_q \tilde{E}_{y,q} \tilde{E}_{y,q}^* d\alpha_n - \int_{-a}^{+a} G_{12}(\alpha_n, \beta) \sum_{p=1}^{\infty} a_p \tilde{E}_{x,p} \tilde{E}_{y,q}^* d\alpha_n \right] = 0, \quad (10.a)$$

$$\left\langle \tilde{j}_x, \tilde{E}_{x,p} \right\rangle = \frac{1}{2a\Delta_G} \left[ \int_{-a}^{+a} G_{22}(\alpha_n, \beta) \sum_{p=1}^{\infty} a_p \tilde{E}_{x,p} \tilde{E}_{x,p}^* d\alpha_n - \int_{-a}^{+a} G_{21}(\alpha_n, \beta) \sum_{q=1}^{\infty} b_q \tilde{E}_{y,q} \tilde{E}_{x,p}^* d\alpha_n \right] = 0. \quad (10.b)$$

Now, a system of compact matrix equations for determining the frequency dependent complex propagation constant  $\beta$  can be obtained

$$\det \begin{bmatrix} M_{q,p}^{1,1}(\beta) & M_{q,q}^{1,2}(\beta) \\ M_{p,p}^{2,1}(\beta) & M_{p,q}^{2,2}(\beta) \end{bmatrix} = 0. \quad (11)$$

The elements of the matrix  $M(\beta)$  are derived from (10) considering the Parseval's theorem [36].

$$M_{q,p}^{1,1}(\beta) = \sum_n \frac{1}{\Delta_G} G_{22}(\alpha_n, \beta) \tilde{E}_{x,p} \tilde{E}_{y,q}^*, \quad (12.a)$$

$$M_{q,q}^{1,2}(\beta) = -\sum_n \frac{1}{\Delta_G} G_{12}(\alpha_n, \beta) \tilde{E}_{y,q} \tilde{E}_{y,q}^*, \quad (12.b)$$

$$M_{p,p}^{2,1}(\beta) = -\sum_n \frac{1}{\Delta_G} G_{21}(\alpha_n, \beta) \tilde{E}_{x,p} \tilde{E}_{x,p}^*, \quad (12.c)$$

$$M_{p,q}^{2,2}(\beta) = \sum_n \frac{1}{\Delta_G} G_{11}(\alpha_n, \beta) \tilde{E}_{y,q} \tilde{E}_{x,p}^*. \quad (12.d)$$

To extract the complex propagation constant  $\beta$  from (11), Muller's root-finding procedure is used.

### 4. Results and Discussions

In order to validate the efficiency of the proposed method, three cases of complex magnetic anisotropy have been calculated. Numerical results are presented in Fig. 2, they show good agreements with literature [37], [38].

In this study, combinations of chiral and achiral bianisotropic medium-based 3-layer CPW (Fig. 1) were considered. The effect of bianisotropic parameters on the complex propagation constant is investigated. New cases of bianisotropic chiral/achiral media are considered using combinations of the imaginary valued magnetoelectric parameters; cases that have not been sufficiently investigated in the literature, especially when  $\xi = \eta$ . This work constitutes a complement and succeeding work of recent research works [1], [26] and especially [23] which dealt with a bianisotropic Tellegen case medium.

In what follows, principal cases of chiral and achiral bianisotropy with diagonal and gyrotropic magnetoelectric parameters are treated.

Two cases for diagonal chiral and achiral bianisotropy:

- $\xi_{ii,1} = ja\sqrt{\varepsilon_r}$  with  $\eta_{ii,1} = -\xi_{ii,1}$ ,
- $\xi_{ii,2} = ja\sqrt{\varepsilon_r}$  with  $\eta_{ii,2} = \xi_{ii,2}$

and six cases for the gyrotropic one ( $\xi_{ij} = ja\sqrt{\varepsilon_r}$ ):

- $\eta_{ij,1} = -\xi_{ij,1}$ ,  $\xi_{ji,1} = \xi_{ij,1}$  and  $\eta_{ji,1} = \eta_{ij,1}$ ,
- $\eta_{ij,2} = \xi_{ij,2}$ ,  $\xi_{ji,2} = \xi_{ij,2}$  and  $\eta_{ji,2} = -\eta_{ij,2}$ ,
- $\eta_{ij,3} = \xi_{ij,3}$ ,  $\xi_{ji,3} = \xi_{ij,3}$  and  $\eta_{ji,3} = \eta_{ij,3}$ ,
- $\eta_{ij,4} = -\xi_{ij,4}$ ,  $\xi_{ji,4} = \xi_{ij,4}$  and  $\eta_{ji,4} = -\eta_{ij,4}$ ,
- $\eta_{ij,5} = -\xi_{ij,5}$ ,  $\xi_{ji,5} = -\xi_{ij,5}$  and  $\eta_{ji,5} = \eta_{ij,5}$ ,
- $\eta_{ij,6} = \xi_{ij,6}$ ,  $\xi_{ji,6} = \xi_{ij,6}$  and  $\eta_{ji,6} = \eta_{ij,6}$

where  $i = x, y, z$  and  $a = -1, -0.75, -0.5, -0.25, 0.25, 0.5, 0.75, 1$ .

As stated above, sign combinations between the magnetoelectric elements are adopted to establish six gyrotropic cases, so that new original results treating the bianisotropic medium as a complex solution can be validated

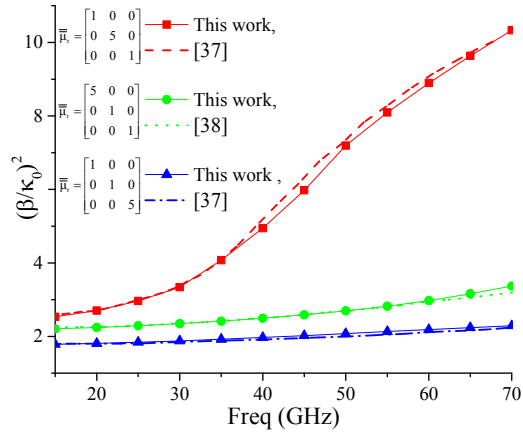


**Fig. 2.**  $(\beta/\kappa_0)^2$  for the dominant mode of a shielded CPW with magnetic anisotropy, ( $2a = 3.556$  mm,  $2w = 2s = 0.7112$  mm,  $d_1 = 2.8448$  mm,  $d_2 = 0.7112$  mm,  $d_3 = 3.556$  mm and  $\epsilon_r = 3$ ).

and compared with the Tellegen case [23]. In this parametric analysis, the effects of diagonal and gyrotropic chiral and achiral elements (imaginary valued magnetoelectric elements) on the complex propagation constant were investigated.

#### 4.1 Effect of the Diagonal Chiral/Achiral Bianisotropy

For diagonal bianisotropy, four (04) cases of magnetoelectric elements are investigated. In Fig. 3, the effects of two cases of the element  $\xi_{yy}$  are presented. A slight difference between the effects of the two cases on the ratio  $(\beta/\kappa_0)^2$  is observed (Fig. 3a), with a reciprocal effect and low losses for Case (i), and a significant coefficient of  $(\alpha/\kappa_0)^2$  for Case (ii) (Fig. 3b) compared to the isotropic case.

In these cases ( $ii = yy$ ) propagating modes are excited in the guiding structure, however, no solutions are obtained for  $ii = xx$  and  $ii = zz$ , hence, the medium with these properties ( $\xi_{ii,1} = ja\sqrt{\epsilon_r}$  with  $\eta_{zz,1} = -\xi_{zz,1}$ ) does not support any

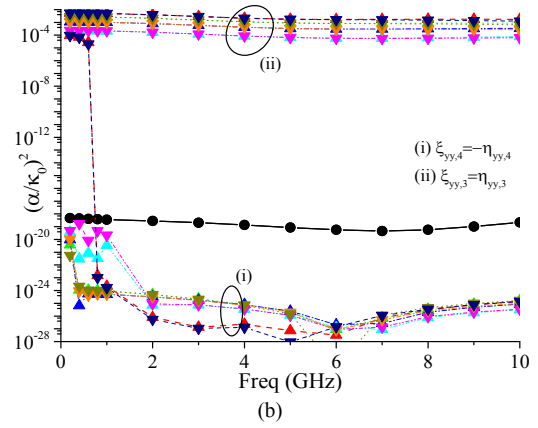
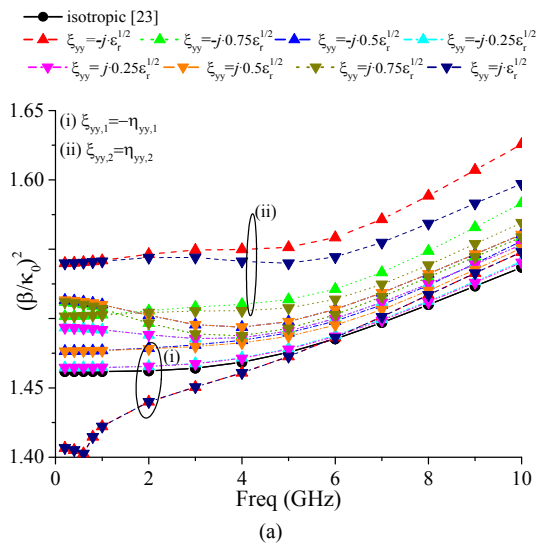


**Fig. 3.** Effect of diagonal chiral/achiral bianisotropy (i)  $\eta_{yy,1} = -\xi_{yy,1}$  and (ii)  $\eta_{yy,2} = \xi_{yy,2}$  on (a):  $(\beta/\kappa_0)^2$  and (b):  $(\alpha/\kappa_0)^2$ .

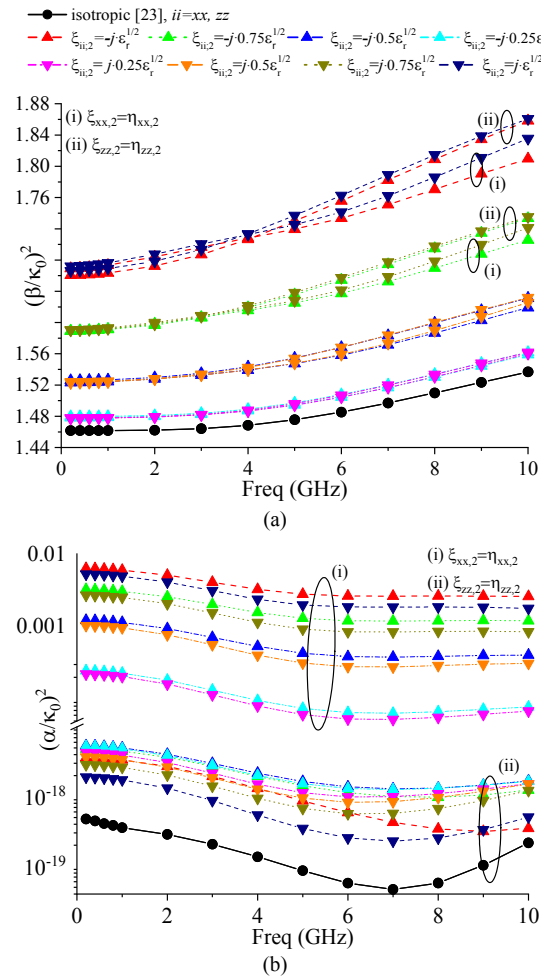


**Fig. 4.** Effect of diagonal chiral/achiral bianisotropy (i)  $\xi_{xx,2}$  with  $\eta_{xx,2} = \xi_{xx,2}$  and (ii)  $\xi_{zz,2}$  with  $\eta_{zz,2} = \xi_{zz,2}$  on (a):  $(\beta/\kappa_0)^2$  and (b):  $(\alpha/\kappa_0)^2$ .

propagating modes, the same result had been obtained for Tellegen media in [23].

Figure 4 illustrates the effect of diagonal bianisotropic media for the case  $\eta_{ii} = \xi_{ii}$ , where  $ii = xx$  or  $zz$ . In this case, the chosen medium is almost reciprocal. For frequencies above 4 GHz and  $\xi_{ii,2} \geq j0.75\sqrt{\epsilon_r}$ , the effects of the  $x$  or  $z$

magnetolectric elements on  $(\alpha/\kappa_0)^2$  are clearly distinct, whereas their effects on  $(\beta/\kappa_0)^2$  are quite similar. The case  $\eta_{zz,2} = \xi_{zz,2}$  demonstrates lower losses (Fig. 4b); this important result is directly related to the tangential and longitudinal distribution fields.

## 4.2 Effect of Gyrotropic Chiral/Achiral Bianisotropy

In Fig. 5a and b, the case  $\xi_{xy,1}$  corresponds to a lossless reciprocal chiral medium case, it is the most commonly treated medium in literature. It can be noticed that for values of  $|\xi_{xy,1}|$  close to  $j\sqrt{\epsilon_r}$ , propagating modes are likely to disappear ( $\beta$  close to zero).

Figures 5c and d show three different combinations of purely imaginary elements compared to a Tellegen case with a purely real element  $\xi_{xy} = 0.75\sqrt{\epsilon_r}$ . The cases of the imaginary valued elements  $\xi_{xy,2}$ ,  $\xi_{xy,3}$  and  $\xi_{xy,4}$  correspond to non-reciprocal gyrotropic media. They differ from each other by a single change of sign between the magneto-electric elements. The reciprocity of the three considered cases decreases with the parameter  $\xi_{xy}$  and frequency compared to the case of real valued element  $\xi_{xy} = 0.75\sqrt{\epsilon_r}$  studied in [23] which inversely increases with frequency. The losses (Fig. 5d) are considerable for these three cases and they are close to the Tellegen case with  $\xi_{xy} = -0.75\sqrt{\epsilon_r}$  for lower frequencies and approaches the case  $\xi_{xy} = 0.75\sqrt{\epsilon_r}$  with increasing frequency.

Results of Fig. 6a–d show reciprocal chiral cases for the elements  $\xi_{xz,1}$ ,  $\xi_{xz,4}$  and  $\xi_{xy,5}$  with significant losses compared to the isotropic case. The effects of  $\xi_{xz,4}$  and  $\xi_{xz,5}$  on both  $(\beta/\kappa_0)^2$  and  $(\alpha/\kappa_0)^2$  are identical: curves are superposed (Fig. 6c and d). These results of chiral cases are compared to a similar Tellegen case [23].

The elements  $\xi_{xz}$  highly affect the ratio  $(\beta/\kappa_0)^2$  for both chiral and Tellegen media cases compared to the isotropic case. The difference is that the Tellegen case shows non-reciprocity and lower losses. Both media show a relative permittivity close to unity for  $a = \pm 0.75$ , with a lower dispersivity which is favorable for radiating structures.

Figures 7a–d present the effect of the element  $\xi_{yz}$ . The chiral in this case ( $\xi_{yz} = -\eta_{yz}$ ) shows a reciprocal effect on  $(\beta/\kappa_0)^2$  (Fig. 7a). This effect is closer to that of the element  $\xi_{xy,1}$  (Fig. 5a). These two elements constitute the longitudinal components that share the y-axis (the direction of propagation) according to the considered geometrical orientation of the studied structure. The only difference lies in the  $(\alpha/\kappa_0)^2$  ratio which is quite different in the two cases. In Fig. 7c, the effect of combinations of the chiral magneto-electric element  $\xi_{yz}$  on  $(\beta/\kappa_0)^2$  is presented. Regardless the element sign change between these cases, the effect on the ratio  $(\beta/\kappa_0)^2$  is quite identical. Compared to the Tellegen case [23], the latter shows non-reciprocity for higher frequencies and lower losses (Fig. 7d).

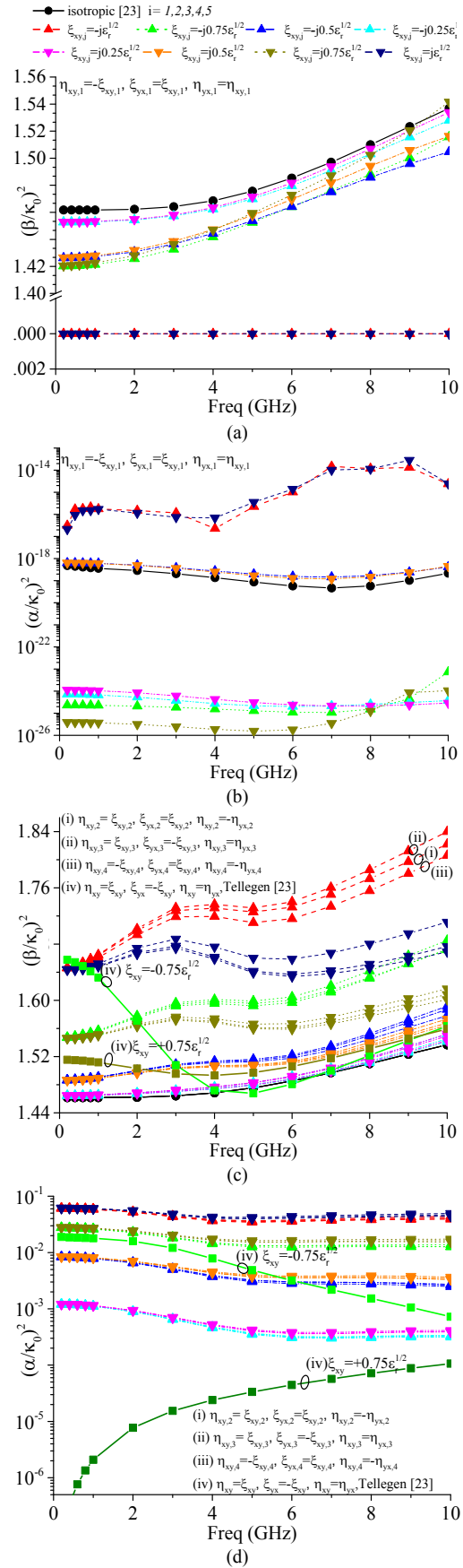


**Fig. 5.** Effect of gyrotropic chiral/achiral bianisotropy for different  $\xi_{xy}$ ,  $\xi_{xz}$ ,  $\eta_{xy}$  and  $\eta_{xz}$  combinations on (a) and (c):  $(\beta/\kappa_0)^2$  and (b) and (d):  $(\alpha/\kappa_0)^2$ .

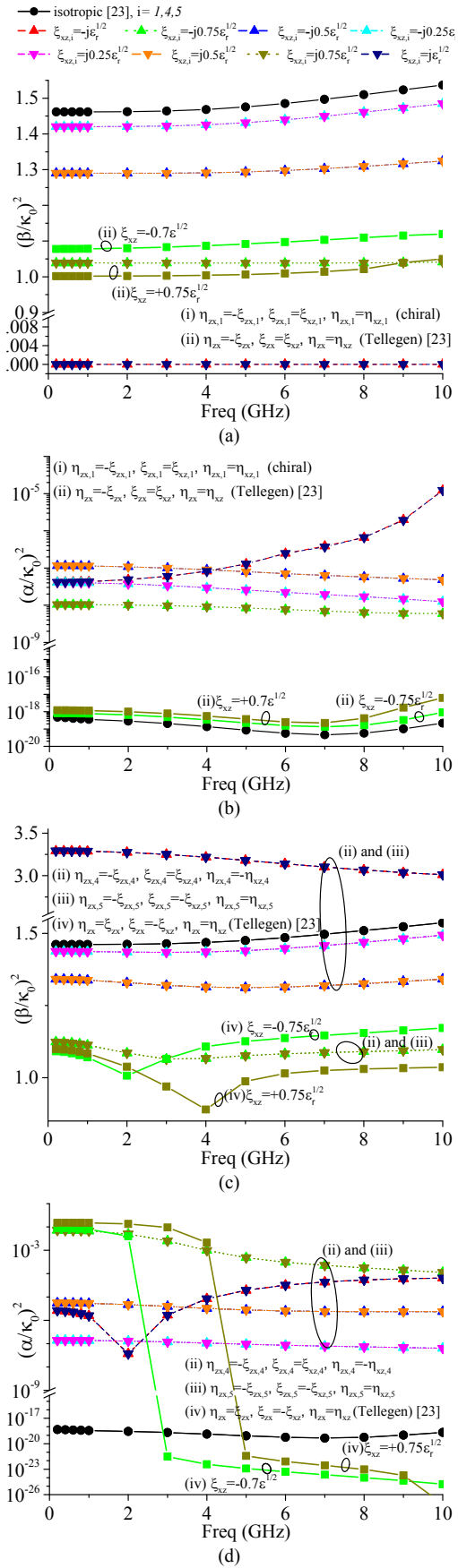


**Fig. 6.** Effect of gyrotropic chiral/achiral bianisotropy for different  $\xi_{xz}$ ,  $\xi_{yz}$ ,  $\eta_{xz}$  and  $\eta_{yz}$  combinations on (a) and (c):  $(\beta/k_0)^2$  and (b) and (d):  $(\alpha/k_0)^2$ .

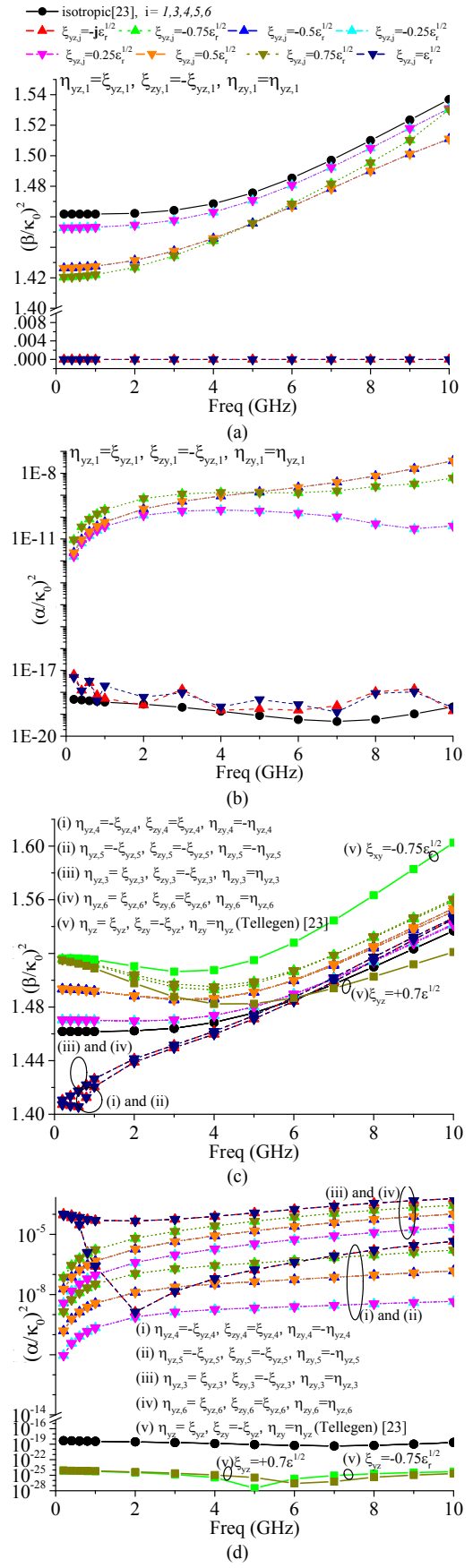


**Fig. 7.** Effect of gyrotropic chiral/achiral bianisotropy for different  $\xi_{yz}$ ,  $\xi_{zy}$ ,  $\eta_{yz}$  and  $\eta_{zy}$  combinations on (a) and (c):  $(\beta/k_0)^2$  and (b) and (d):  $(\alpha/k_0)^2$ .

## 5. Conclusion

In this work, an analytical modeling of a 3-layer suspended CPW implanted on a bianisotropic substrate is presented. The study is based on the Full-GEMT developed in a matrix form for the characterization of a bianisotropic medium CPW structure for the calculation of the complex propagation constant.

According to calculations, cases of complex media with a relative effective permittivity close to unity were obtained, such as for cases  $\xi_{xz,1}$ ,  $\xi_{xz,4}$  and  $\xi_{xz,5}$ . The same results had been obtained with Tellegen media except that losses are significant for the cases of  $\xi_{xz,4}$  and  $\xi_{xz,5}$  and moderate in the case of  $\xi_{xz,1}$ . This characteristic is important for the realization of media with weak relative permittivity for better use in the design of filtering and radiating structures. Moreover, lower dispersivity is attained for these cases, which is favorable for wideband microwave structure applications.

In the case of  $\xi_{xy}$  the difference between the chiral and achiral media is quite remarkable. The chiral medium presents lower losses compared to achiral. The same remark is true for the element  $\xi_{yz}$  losses are higher than the isotropic case.

On the other hand, losses in chiral and achiral media increase in some cases and considerably decrease in others along with the sign change of the magnetoelectric elements combinations, this should be taken into consideration. Moreover, it is worth noting that the transverse components  $\xi_{xz}$  are the most influential on the phase constant, whether in chiral or achiral media, this is mainly due to the geometrical orientation of the studied structure. Finally, this study constitutes an advanced bianisotropic model for the characterization of microwave devices that can be relied on as a base on which novel modeling techniques can be built.

## Acknowledgments

This work is also funded by the FCT/MEC through national funds and when applicable co-financed by the ERDF, under the PT2020 Partnership Agreement under the UID/EEA/50008/2019 project.

## References

- [1] SAYAD, D., ZEBIRI, C., DAOUDI, S., et al. Analysis of the effect of a gyrotropic anisotropy on the phase constant and characteristic impedance of a shielded microstrip line. *Advanced Electromagnetics*, 2019, vol. 8, no. 5, p. 15–22. DOI: 10.7716/aem.v8i5.946
- [2] SHELBY, R. A., SMITH, D. R., SCHULTZ, S. Experimental verification of a negative index of refraction. *Science*, 2001, vol. 292, no. 5514, p. 77–79. DOI: 10.1126/science.1058847
- [3] BILOTTI, F., SEVGI, L. Metamaterials: Definitions, properties, applications, and FDTD-based modeling and simulation. *International Journal of RF and Microwave Computer-Aided Engineering*, 2012, vol. 22, no. 4, p. 422–438. DOI: 10.1002/mmce.20634
- [4] CHEN, L. F., ONG, C. K., NEO, C. P., et al. *Microwave Electronics: Measurement and Materials Characterization*. 1<sup>st</sup> ed. John Wiley & Sons, 2004. ISBN: 978-0470844922
- [5] MACKAY, T. G., LAKHTAKIA, A. Negatively refracting chiral metamaterials: A review. *SPIE Reviews*, 2010, vol. 1, no. 1, p. 1–29. DOI: 10.1117/6.0000003
- [6] MOLINA-CUBEROS, G. J., GARCIA-COLLADO, A. J., MARGINEDA, J., et al. Electromagnetic activity of chiral media based on crank inclusions. *IEEE Microwave and Wireless Components Letters*, 2009, vol. 19, no. 5, p. 278–280. DOI: 10.1109/LMWC.2009.2017588
- [7] LINDELL, I. V., SIHVOLA, A. H., VIITANEN, A. J., TRETYAKOV S. A. *Electromagnetic Waves in Chiral and Bi-isotropic Media*. Artech House, 1994. ISBN: 0890066841
- [8] SIHVOLA, A., SEMCHENKO, I., KHAKHOMOV, S. View on the history of electromagnetics of metamaterials: Evolution of the congress series of complex media. *Photonics and Nanostructures-Fundamentals and Applications*, 2014, vol. 12, no. 4, p. 279–283. DOI: 10.1016/j.photonics.2014.03.004
- [9] NOVITSKY, A., SHALIN, A. S., LAVRINENKO, A. V. Spherically symmetric inhomogeneous bianisotropic media: Wave propagation and light scattering. *Physical Review A*, 2017, vol. 95, no. 5, p. 1–11. DOI: 10.1103/PhysRevA.95.053818
- [10] ASADCHY, V. S., DÍAZ-RUBIO, A., TRETYAKOV, S. A. Bianisotropic metasurfaces: Physics and applications. *Nanophotonics* 2018, vol. 7, no. 6, p. 1069–1094. DOI: 10.1515/nanoph-2017-0132
- [11] MULJAROV, E. A., WEISS, T. Resonant-state expansion for open optical systems: Generalization to magnetic, chiral, and bianisotropic materials. *Optics Letters*, 2018, vol. 43, no. 9, p. 1978–1981. DOI: 10.1364/OL.43.001978
- [12] KAMRA, V., DREHER, A. Efficient analysis of multiple microstrip transmission lines with anisotropic substrates. *IEEE Microwave and Wireless Components Letters*, 2018, vol. 28, no. 8, p. 636–638. DOI: 10.1109/LMWC.2018.2847032
- [13] BUZOV, A. L., BUZOVA, M. A., KLYUEV, D. S., et al. Calculating the input impedance of a microstrip antenna with a substrate of a chiral metamaterial. *Journal of Communications Technology and Electronics*, 2018, vol. 63, no. 11, p. 1259–1264. DOI: 10.1134/S1064226918110037
- [14] KLYUEV, D. S., MINKIN, M. A., MISHIN, D. V., et al. Characteristics of radiation from a microstrip antenna on a substrate made of a chiral metamaterial. *Radiophysics and Quantum Electronics*, 2018, vol. 61, no. 6, p. 445–455. DOI: 10.1007/s11141-018-9906-3
- [15] ZHOU, Z., KELLER, S. M. The application of least-squares finite-element method to simulate wave propagation in bianisotropic media. *IEEE Transactions on Antennas and Propagation*, 2019, vol. 67, no. 4, p. 2574–2582. DOI: 10.1109/TAP.2019.2893182
- [16] ZEBIRI, C., LASHAB, M., BENABDELAZIZ, F. Effect of anisotropic magneto-chirality on the characteristics of a microstrip resonator. *IET Microwaves, Antennas & Propagation*, 2010, vol. 4, no. 4, p. 446–452. DOI: 10.1049/iet-map.2008.0439
- [17] HASAR, U. C., BARROSO, J. J., SABAH, C., et al. Stepwise technique for accurate and unique retrieval of electromagnetic properties of bianisotropic metamaterials. *Journal of Optical Society of America B, Optical Physics*, 2013, vol. 30, no. 4, p. 1058–1068. DOI: 10.1364/JOSAB.30.001058

- [18] HASAR, U. C., BULDU, G., Y. KAYA, Y., et al. Determination of effective constitutive parameters of inhomogeneous metamaterials with bianisotropy. *IEEE Transactions on Microwave Theory and Techniques*, 2018, vol. 66, no. 8, p. 3734–3744. DOI: 10.1109/TMTT.2018.2846726
- [19] ZEBIRI, C., LASHAB, M., BENABDELAZIZ, F. Rectangular microstrip antenna with uniaxial bianisotropic chiral substrate-superstrate. *IET Microwaves, Antennas & Propagation*, 2011, vol. 5, no. 1, p. 17–29. DOI: 10.1049/iet-map.2009.0446
- [20] AIB, S., BENABDELAZIZ, F., ZEBIRI, C., et al. Propagation in diagonal anisotropic chirowaveguides. *Advances in OptoElectronics*, 2017, p. 1–8. DOI: 10.1155/2017/9524046
- [21] ZEBIRI, C., DAOUDI, S., BENABDELAZIZ, F., et al. Gyrochirality effect of bianisotropic substrate on the operational of rectangular microstrip patch antenna. *International Journal of Applied Electromagnetics and Mechanics*, 2016, vol. 51, no. 3, p. 249–260. DOI: 10.3233/JAE-150141
- [22] ZEBIRI, C., LASHAB, M., BENABDELAZIZ, F. Asymmetrical effects of bi-anisotropic substrate-superstrate sandwich structure on patch resonator. *Progress In Electromagnetics Research B*, 2013, vol. 49, p. 319–337. DOI: 10.2528/PIERB13012115
- [23] SAYAD, D., ZEBIRI, C., ELFERGANI, I., et al. Complex bianisotropy effect on the propagation constant of a shielded multilayered coplanar waveguide using improved full generalized exponential matrix technique. *Electronics*, 2020, vol. 9, no. 2, p. 1–18. DOI: 10.3390/electronics9020243
- [24] VEGNI, L., TOSCANO, A. Shielding and radiation characteristics of cylindrical layered bianisotropic structures. *Radioengineering*, 2005, vol. 14, no. 4, p. 68–74. ISSN: 1210-2512
- [25] YIN, W. Y., LI, L. W., LEONG, M. S. Hybrid effects of gyrotropy and chirality in chiral-ferrite fin lines. *Microwave and Optical Technology Letters*, 2000, vol. 25, no. 1, p. 40–44. DOI: 10.1002/(SICI)1098-2760(20000405)25:1<40::AID-MOPI2>3.0.CO;2-N
- [26] ZEBIRI, C., SAYAD, D. Effect of bianisotropy on the characteristic impedance of a shielded microstrip line for wideband impedance matching applications. *Waves in Random and Complex Media*, 2020, p. 1–14. DOI: 10.1080/17455030.2020.1752957
- [27] DAOUDI, S., BENABDELAZIZ, F., ZEBIRI, C., et al. Generalized exponential matrix technique application for the evaluation of the dispersion characteristics of a chiro-ferrite shielded multilayered microstrip line. *Progress In Electromagnetics Research M*, 2017, vol. 61, p. 1–14. DOI: 10.2528/PIERM17082107
- [28] TSALAMENGAS, J. L. Interaction of electromagnetic waves with general bianisotropic slabs. *IEEE Transactions on Microwave Theory and Technique*, 1992, vol. 40, no. 10, p. 1870–1878. DOI: 10.1109/22.159623
- [29] XU, H., JAIN, S., SONG, J., et al. Acceleration of spectral domain immittance approach for generalized multilayered shielded microstrips using the Levin's transformation. *IEEE Antennas and Wireless Propagation Letters*, 2014, vol. 14, p. 92–95. DOI: 10.1109/LAWP.2014.2356401
- [30] OUESLATI, N., AGUILI, T. An improved MoM-GEC method for fast and accurate computation of transmission planar structures in waveguides: Application to planar microstrip lines. *Progress In Electromagnetics Research M*, 2016, vol. 48, p. 9–24. DOI: 10.2528/PIERM16030204
- [31] SAYAD, D., BENABDELAZIZ, F., ZEBIRI, C., et al. Spectral domain analysis of gyrotropic anisotropy chiral effect on the input impedance of a printed dipole antenna. *Progress In Electromagnetics Research M*, 2016, vol. 51, p. 1–8. DOI: 10.2528/PIERM16073106
- [32] LUCIDO, M. A new high-efficient spectral-domain analysis of single and multiple coupled microstrip lines in planarly layered media. *IEEE Transactions on Microwave Theory and Techniques*, 2015, vol. 60, no. 7, p. 2025–2034. DOI: 10.1109/TMTT.2012.2195025
- [33] JAIN, S., SONG, J., KAMGAING, T., et al. Acceleration of spectral domain approach for generalized multilayered shielded microstrip interconnects using two fast convergent series. *IEEE Transactions on Components, Packaging and Manufacturing Technology*, 2013, vol. 3, no. 3, p. 401–410. DOI: 10.1109/TCPMT.2012.2222644
- [34] VAN BLADEL, J. G. *Electromagnetic Fields*. 2<sup>nd</sup> ed. Wiley-IEEE Press, 2007. ISBN: 978-0-471-26388-3
- [35] CHIANG, K. S. Review of numerical and approximate methods for the modal analysis of general optical dielectric waveguides. *Optical and Quantum Electronics*, 1994, vol. 26, no. 3, p. S113–S134. DOI: 10.1007/BF00384667
- [36] MIRSHEKAR-SYAHKAL, D. *Spectral Domain Method for Microwave Integrated Circuits*. Wiley-Blackwell, 1990. ISBN: 0863800998
- [37] MAZE-MERCEUR, G., TEDJINI, S., BONNEFOY, J. L. Analysis of a CPW on electric and magnetic biaxial substrate. *IEEE Transactions on Microwave Theory and Technique*, 1993, vol. 41, no. 3, p. 457–461. DOI: 10.1109/22.223745
- [38] KHODJA, A., YAGOUB, M. C. E., TOUHAMI, R., et al. Practical recurrence formulation for composite substrates: Application to coplanar structures with bi-anisotropic dielectrics. In *Proceedings of the 18th Mediterranean Microwave Symposium (MMS)*. Istanbul (Turkey), 2018, p. 341–344. DOI: 10.1109/MMS.2018.8612139

## About the Authors ...

**Djamel SAYAD** received the Ph.D. degree in Electronics from the University of Skikda, Algeria, in 2017. He is currently an Associate Professor with the Department of Electrical Engineering, University of Skikda. His current research interests include electromagnetics and complex media, and microwave propagation and antennas.

**Chemseddine ZEBIRI** received the Ph.D. degree in Electronics from the University of Constantine, Algeria, in 2011. He has been with the Department of Electronics, University of Ferhat Abbas, Setif, Algeria, since 2006, where he is currently an Associate Professor. He started working on reflector, microstrip antennas and transmission lines printed on anisotropic medium using the MoM in time and spectral domains. He has published up to 100 journal and refereed conference articles. He is the author of four book chapters. His current research interests include dielectric resonator antennas, MIMO antennas, mm-Wave antennas, chiral and magnetic materials, and microwave and optical complex material components.

**Issa T. E. ELFERGANI** (corresponding author) received the M.Sc. and Ph.D. degrees in Electrical and Electronic Engineering from the University of Bradford, U.K., in 2008 and 2012, respectively, with a specialization in tunable antenna design for mobile handset and UWB applications. He is currently a Senior Researcher with the Instituto de Telecomunicações, Campus Universitário de Santiago, Aveiro, Portugal, working in several national and interna-

tional research funded projects. He has around 125 high-impact publications in academic journals and international conferences. In addition, he is the author of two book editorials and nine book chapters.

**Jonathan RODRIGUEZ** received the master's degree in Electronic and Electrical Engineering and the Ph.D. degree from the University of Surrey, U.K., in 1998 and 2004, respectively. In 2005, he became a Researcher with the Instituto de Telecomunicações, Campus Universitário de Santiago, Portugal, where he was a member of the Wireless Communications Scientific Area. In 2008, he became a Senior Researcher and established the 4TELL Research Group targeting next-generation mobile systems. He has served as a Project Coordinator for major international research projects. Since 2009, he has been served as an Invited Assistant Professor with the University of Aveiro, Portugal, and attained associate level, in 2015. In 2017, he was an Appointed Professor of mobile communications with the University of South Wales, U. K. He is the author of more than 400 scientific works, including ten book editorials. His professional affiliations include a chartered engineer (C.Eng.) (2013) and a Fellow of the IET, in 2015.

**Raed A. ABD-ALHAMEED** (M'02–SM'13) received the B.Sc. and M.Sc. degrees from Basrah University, Basrah, Iraq, in 1982 and 1985, respectively, and the Ph.D. degree from the University of Bradford, West Yorkshire, U.K., in 1997. He is a Professor in Electromagnetic and Radio Frequency Engineering with the University of Bradford, U.K. He has long years' research experience in the areas of radio frequency, signal processing, propagations, and antennas and electromagnetic computational techniques. He has published over 600 academic journal and conference articles. In addition, he is the coauthor of four books and several book chapters. He is the Fellow of the Institution of Engineering and Technology and the Higher Education Academy, and a Chartered Engineer.

**Fatiha BENABDELAZIZ** received her Ph.D degree in 1986 from Moscow Technical University of Communications and Informatics. She is currently a professor with the Department of Electronics, University of Constantine 1, Algeria. She has published more than 100 journal and refereed conference articles. Her current research interests include optics, electromagnetics and complex media, microwave propagation and antennas.